EFFECT OF CERIUM SALT ACTIVATED CERIA ON THE UV DEGRADATION RESISTANCE OF WATERBORNE EPOXY COATINGS

Thuy Duong Nguyen, Thu Thuy Thai, Anh Son Nguyen[*]

*Institute for Tropical Technology, Vietnam Academy of Science and Technology
A13 Building, 18 Hoang Quoc Viet, Cau Giay District, Ha Noi, Viet Nam*

[*]Email: *nason@itt.vast.vn*

Abstract. Ce (III) salt-activated CeO_2 nanoparticles were incorporated into waterborne epoxy coating to improve the UV stabilisation of epoxied system. The surface morphology of the coatings was examined by using color spectrophotometer during the UV exposure test. The degradation of the epoxy coatings was observed by the change of barrier property determined by electrochemical impedance spectroscopy. The effect of activated nanoparticles on the impact resistance and adherence properties was also evaluated by impact strength test and cross-cut test. The results showed that the epoxy coating with the presence of Ce^{3+}/CeO_2 nanoparticles loss only 9.5 % discoloration compared to the non-aged coatings. After 28 cycles of UV test, the barrier property of this coating can be maintained at high impedance module value at low frequency. The epoxy-Ce^{3+}/CeO_2 also presented a good impact strength value, 160 kg.cm, at the end of UV test. On the other hand, the presence of the inorganic compound in the epoxy matrix did not affect to adherence property of polymer system before or after UV irradiation exposure test.

Keywords: Ceria nanoparticles, cerium salt-activated, waterborne epoxy coatings, UV degradation.

Classification numbers: 2.4.4, 2.5.3, 2.9.3.

1. INTRODUCTION

Epoxies have been widely used as protective coating for numerous materials due to their excellent mechanical properties, chemical resistance, good electrical insulating properties and strong adhesion [1, 2]. Depending on the application, some organic/inorganic additives have been added to enhance the corresponding properties such as anticorrosion, adherence, electrical conductivity, etc. [3 - 8]. However, the epoxy coatings usually degrade under UV irradiation that induce the decreases of their physical and chemical properties such as discoloration or chalking [9, 10]. For this reason, the use of the epoxy resin is limited in the outdoor applications, or the epoxy coatings must be applied onto the substrate as a primer coating with a top coating, which can resist the UV light.

To stabilize the epoxy resin in the presence of UV, many works had been realized with the incorporation of some antioxidants or photo-stabilizers into polymer matrix. Zhang *et al*. [11] had inserted a light stabilizer containing 2,2,6,6-tetramethylpiperidine functional group into the interlayer region of Mg-Al layered double hydroxides (LS-LDH) to improve environmental resistance of polypropylene (PP). With 4 wt. % of loading compounds, the PP/LS-LDH presented an excellent anti-ageing (thermal and photo stability) performance, compared to PP/CO$_3$-LDH. However, the organic compounds could react to polymer matrix that affect on the polymer structure and to change physical and/or chemical properties of the system. On the other hand, inorganic additives have been used to improve photo degradation resistance of polymers, such as zinc oxide (ZnO), titanium oxide (TiO$_2$) or carbon black (CB) [12 - 14]. Ghasemi-Kahrizsangi *et al*. [15] demonstrated that the epoxy coating containing 2.5 wt. % of CB loading displayed no microcracks after 1000 h of UV exposure. In addition, this coating generated much less carbonyl group (from chain scission) than that of neat epoxy coating. Nevertheless, the CB particles are well-known to easily tend to agglomeration or clusters, that is difficult to disperse in the polymer matrix.

In recent years, cerium (IV) oxide (ceria, CeO$_2$) nanoparticles became a candidate to replace the traditional antioxidants and photostabilizers because they can absorb UV irradiation without any photoactive effects [16]. This characteristic is due to the rapid recombination of charge carriers before they can migrate to the surface of the particles. Dao *et al*. [17] showed that the epoxy nanocomposite containing 1 wt. % CeO$_2$ could absorb more than 90 % of UV irradiation and presented an increase of 3 % of tensile strength, compared to neat epoxy resin. For better dispersing the nanoparticles in the polymer matrix, the nano CeO$_2$ could be activated on the surface by the metals form cations such as: cobalt, cerium, etc. [16, 18]. The results showed that the activated nanoparticles could enhance both anticorrosion and mechanical properties of the organic coatings.

This work was focused on the UV degradation resistance of waterborne epoxy coatings containing cerium salt activated ceria nanoparticles. The surface morphology and the barrier property of the coatings were observed during the UV exposure test by the color spectrophotometer and the electrochemical impedance spectroscopy (EIS). Thus, the impact resistance and adherence property of the coatings before and after UV exposure were measured to completely evaluate the UV-blocked ability of the activated nanoparticles for epoxy matrix.

2. MATERIALS AND METHODS

2.1. Materials and samples preparation

The coating used in this study was a commercial bicomponent water-based epoxy system. The base was a bisphenol A epoxy resin - Epikote 828 provided by Hexion (Thailand) that has equivalent weight of about 184 - 190 g/eq. Epikure 8537-wy-60 produced by Momentive (Thailand) was used as a hardener which has an amine value of 310-360 mg/g and an equivalent weight of 174 g/eg. It was a water-reducible amine adducts consisted of 60 wt. % solids in water, 2-propoxyethanol and glacial acetic acid.

Cerium (III) nitrate hexahydrate (Ce(NO$_3$)$_3$.6H$_2$O) and ammonia solution were purchased from Merck to synthesize CeO$_2$ nanoparticles and to prepare cerium (III) activated ceria nanoparticles (Ce^{3+}/CeO$_2$) by the same methods already described in reference [18]. For the coating nanocomposites, the prepared CeO$_2$ and Ce^{3+}/CeO$_2$ nanoparticles were slowly added into the hardener solution with strongly stirred by magnetic stirring and ultrasonicated by T10 IKA

dispersers, Ultra-Turrax (water was adjusted to receive a mixture with similar viscosity for all samples). The obtained suspensions were added epoxy resin with stoichiometry ratio into and stirred for 1 h. The epoxy-CeO_2 and epoxy-Ce^{3+}/CeO_2 were then applied onto the carbon steel XC 35 plate with size of $150 \times 100 \times 1$ mm by spin coating technique with 600 rpm for 10 s. After drying a week in air, the sample thickness was 30 ± 3 μm (measured by Minitest 600 Erichen digital meter).

2.2. Analytical methods

The UV absorption of CeO_2 and Ce^{3+}/CeO_2 nanoparticles was recorded on UV - Vis S80 Libra (Biochrom) spectrophotometer in the spectral range from 250 to 500 nm with a double-beam optical spectrum analyzer. The nanoparticles were dispersed at 10 ppm in distilled water by ultrasonication for 15 mins. The morphology of the different nanoparticles was observed by Transmission Electron Microscope (TEM), JEM-T8 at 80 kV.

The UV exposure test was carried out using a UV-condensation chamber Atlas UVCON UC-327-2 with fluorescent UV lamps UVB 313 according to ASTM G53-96. The condition for each cycle was set for 8 h of UV exposure and 4 h of condensation.

The morphology of the additives in the epoxy matrix was studied by Field Emission Scanning Electron Microscope, Hitachi S-4800. The observed zones of all samples were taken at the cross-section with an acceleration voltage of 5 kV.

The surface morphology of the coatings was characterized by color spectrophotometer (CI6X X-rite). The total color difference as a function of UV exposure cycle was determined according to the equation:

$$\Delta E = \sqrt{(L_2 - L_1)^2 + (a_2 - a_1)^2 + (b_2 - b_1)^2} \qquad (1)$$

where L, a and b indicate lightness, the red/green coordinate and the yellow/blue coordinate, respectively.

Attenuated Total Reflection-Fourier Transform Infrared Spectroscopy (ATR-FTIR) was performed to observe the chemical bonds which were varied after the UV irradiation exposure. All samples were measured in air at room temperature using Nicolet iS10, Thermo Scientific equipment. The measurements were in range from 4000 to 400 cm^{-1} with the 8 cm^{-1} of resolution. The carbonyl index (CI) was calculated using the following formula [15]:

$$CI = I_c/I_m \qquad (2)$$

where, I_c, I_m are intensity of absorbance peaks corresponded to carbonyl and methyl groups, respectively.

The barrier property of the epoxy coatings containing CeO_2 or Ce^{3+}/CeO_2 nanoparticles were explored by EIS technique with Biologic Potentiostat VSP-300. Before each measurement, the electrolyte (0.5 M Na_2SO_4 solution) was filled into a fixed cylindrical tube on top of the samples. After 2 h for stabilizing system, the impedance measurements were performed at the open circuit potential (OCP) over a frequency range of 100 kHz to 10 mHz, applied an amplitude of 30 mV with 8 points per decade. At least three different times were measured each sample to ensure the reproducibility.

The impact resistance of the samples was determined according to ASTM D2794. The values of impact resistance were obtained with maximum height of standard weight (2 kg) dropped on the surface of samples, and no fracture was observed at the contact zone. The adherence property of epoxy nanocomposite coatings was characterized by cross-cut method

according to ASTM D 3359 with the crosshatch cutter six blades (1 mm spaces between cutting edges).

3. RESULTS AND DISCUSSION

3.1. Effect of synthetized nanoparticles on the UV absorption property

Figure 1 shows the UV absorbance spectra of both synthesized CeO_2 and Ce^{3+}/CeO_2 nanoparticles. The absorption maxima of CeO_2 was determined at 306 nm, while that of Ce^{3+}/CeO_2 was observed at 298 nm. Moreover, the TEM micrographs showed that the agglomeration of the hexagonal CeO_2 particles is less important for the activated nanoparticles. These results confirm that the slight shift of the UV absorption maxima is due to the different size of particles, this hypothesis was also demonstrated by Kumar *et al*. [19].
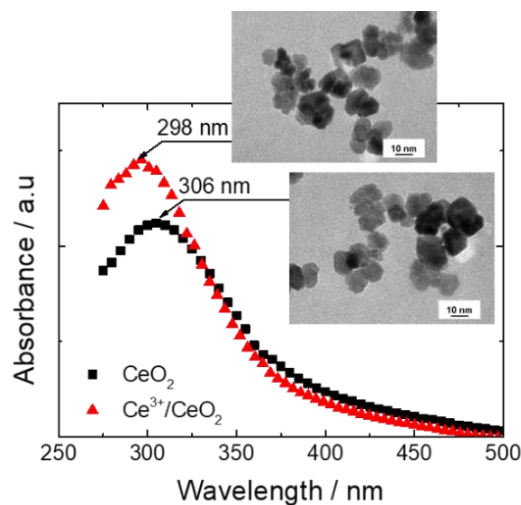

Figure 1. UV-visible spectra of CeO_2 (■) and Ce^{3+}/CeO_2 (▲) nanoparticles.
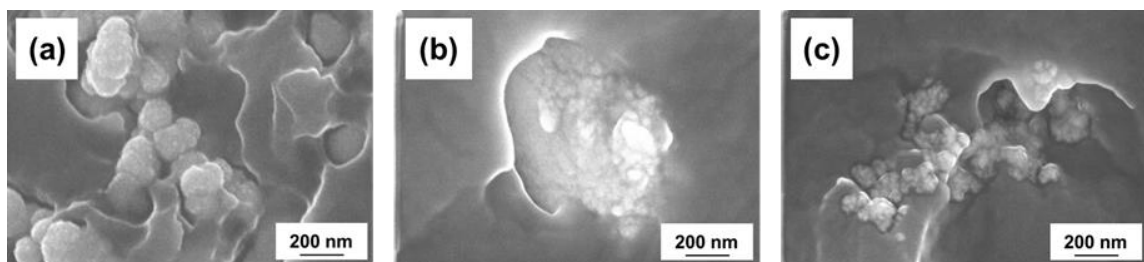
3.2. Morphology of the coatings

Figure 2. Cross-section FESEM micrographs of Epoxy-Ce^{3+} (a), Epoxy-CeO_2 (b) and Epoxy-Ce^{3+}/CeO_2 (c).

The cross-section FESEM micrographs of epoxy coatings containing different additive were shown in Fig. 2. The Epoxy-Ce^{3+} presents an incompatible between $Ce(NO_3)_3$ salts and epoxy matrix. For the coating containing CeO_2, the agglomeration important of the ceria nanoparticles is observed with a particle size of around 500 nm. In contrast, the Fig. 2b

demonstrates a better dispersion and less agglomeration of the cerium (III) ions activated ceria nanoparticles. The morphology will affect on the properties of the coatings.

3.3. Color measurement of the coatings

For epoxy coating, the color difference is one of the most interesting parameters that can clearly illustrate the UV resistance of the system. Due to the yellow color of the CeO_2 nanoparticles, it is difficult to observe the yellowing phenomenon of epoxy under UV irradiation exposure. Fortunately, the UV degradation of epoxy resin will decrease the brightness of the coating. Fig. 3a shows that the difference in lightness of all samples significantly decreased in the first 2 cycles of exposure due to the degradation of epoxy resin and the non-fully-presented CeO_2 nanoparticles on the surface of coatings. Then, the epoxy-Ce^{3+}/CeO_2 presents a slight decrease of brightness until the end of the test. After 28 UV irradiation cycles, the difference in lightness parameter for the epoxy-Ce^{3+}/CeO_2 was around 3 %, while that for the other coatings varied from 4 to 5 %, compared to non-aged coatings. The epoxy-CeO_2 displayed a similar brightness level to the neat epoxy and epoxy-Ce^{3+}, it can be due to its agglomeration in the epoxy matrix.
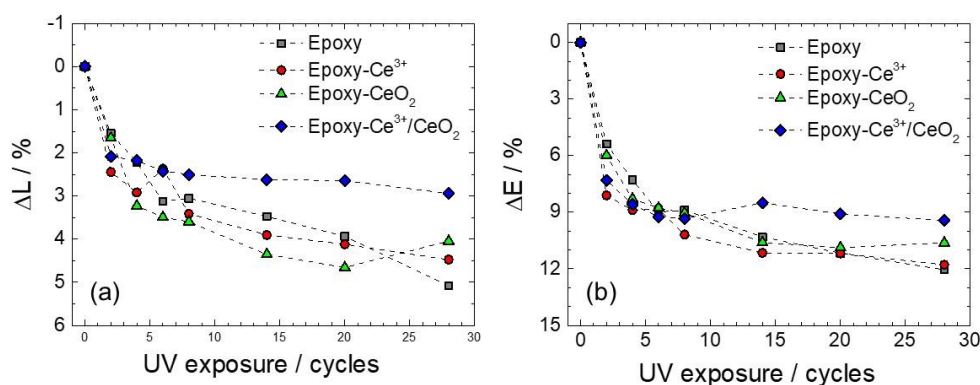

Figure 3. The lightness (a) and color (b) difference of the epoxy coatings containing different additives (as indicated on the figure)**.**

Comparing the total color difference of the samples (Fig. 3b), there is no significant difference after 8 exposure cycles because of the similar color of the nanoparticles and the yellowing phenomenon of aged epoxy resin. But, at the end of the test, it can be observed the UV blocked capacity of CeO_2 nanoparticles with 9.5 %, 10.8 %, 11.9 % and 12.1 % for the epoxy-Ce^{3+}/CeO_2, epoxy-CeO_2, epoxy-Ce^{3+} and neat epoxy, respectively.

3.4. FTIR spectra of the coatings

The changing of color for the tested coatings can be explained by the chemical bond breaking of epoxy matrix during the UV exposure. Figure 4 shows the FTIR spectra of epoxy before and after aging process, as an example. It illustrates that the decrease of the reflectance band at 2855 cm^{-1} and the increase of peak at 1740 cm^{-1}, that correspond to methyl (C-CH_3) and carbonyl (C=O) groups, respectively. It can be explained by the degradation of the C-CH_3 groups during the UV exposure test, that produced the C=O groups in the presence of oxygen [15].
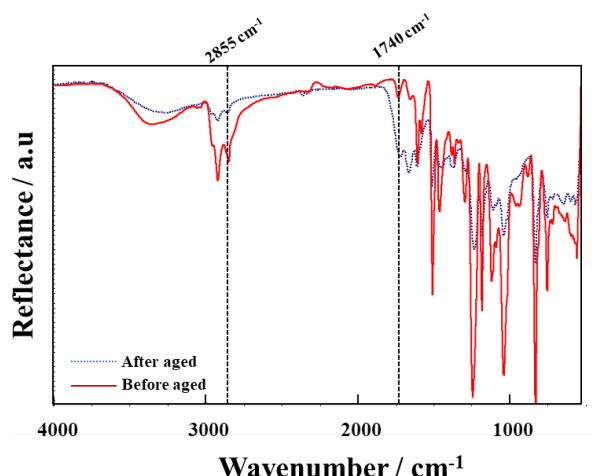
Figure 4. ATR-FTIR spectra of the epoxy without additives obtained before and after 28 cycles of the UV irradiation exposure (indicated on the figure).

The degree of the methyl group degradation will be evaluated by carbonyl index (CI). Table 1 shows that the CI variation of epoxy is similar with that of epoxy-Ce^{3+}, while, in the presence of ceria nanoparticles, the CI values of the epoxy-CeO_2 and epoxy-Ce^{3+}/CeO_2 are less important after the UV irradiation exposure. This result is in agreement with the obtained lightness values for the tested coatings.

Table 1. Carbonyl index of the epoxy coatings containing Ce^{3+}, CeO_2, Ce^{3+}/CeO_2 and neat epoxy coating obtained before and after the UV exposure test.

Sample	Carbonyl Index (CI)	
	0 cycle	28 cycles
Epoxy	0.12	6.10
Epoxy-Ce^{3+}	0.12	6.00
Epoxy-CeO_2	0.12	5.33
Epoxy-Ce^{3+}/CeO_2	0.13	2.06

3.5. Barrier property of the coatings

Figure 5 displays the electrochemical impedance diagrams (in Nyquist format) obtained before UV exposure test for the epoxy coatings with and without photostabilizer. The barrier property of each sample can be determined by extrapolation impedance value at low frequency. The result shows that, at initial state, all coatings presented a high barrier property with a resistance superior to 1.0×10^7 Ω cm^2. In the presence of the nanoparticles, the barrier property of the epoxy coating is improved from 2.6×10^7 to 5.4×10^7 Ω cm^2 due to barrier effect of CeO_2 that improved the coating density. The epoxy-Ce^{3+} had only 2.1×10^7 Ω cm^2 because of the dissolution of $Ce(NO_3)_3$ in the electrolyte solution.
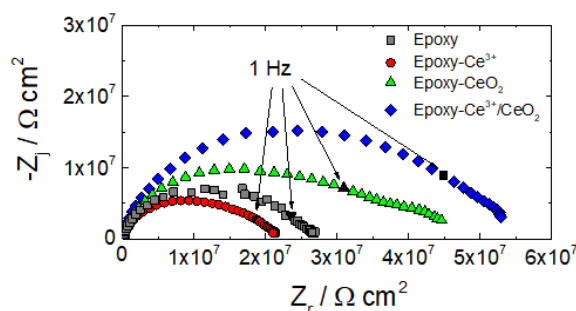
Figure 5. Impedance response in Nyquist format for the waterborne epoxy coatings containing different additives (as indicated on the figure) before UV exposure test.
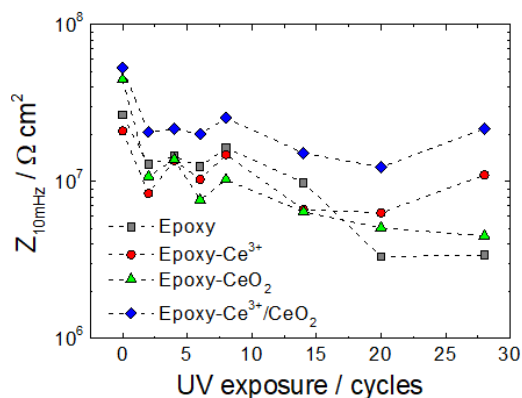

Figure 6. Impedance modulus value measured at 10 mHz as function of UV exposure cycles for different coating systems (indicated on the figure).

To follow the change of barrier property of the coatings under UV irradiation test, the impedance modulus at low frequency (10 mHz) is plotted versus UV exposure cycles (Fig. 6). At the first 2 cycles, a decrease of Z_{10mHz} appears for all coatings because of the degradation of epoxy resin on the surface (as discussed above). Between 2 and 8 cycles, it is observed that all system slightly varied, it can be explained by the continuation of the UV degradation phenomenon on the surface of the coatings. After 8 cycles, the Z_{10mHz} of epoxy-Ce^{3+}/CeO_2 remains stable about 2.1×10^7 Ω cm^2 due to the presence of activated-CeO_2 well-dispersion in the epoxy matrix. The epoxy-CeO_2 presented a bad UV stability like neat epoxy. After 28 cycles, their values of Z_{10mHz} were around $3.0 \div 4.0 \times 10^6$ Ω cm^2. These results obtained by electrochemical measurements are in agreement with the color measurements.

3.6. Mechanical properties

Figure 7 displays the UV blocked effect of $Ce(NO_3)_3$, CeO_2 and Ce^{3+}/CeO_2 pigments on the impact resistance of waterborne epoxy coatings. It shows that the presence of the nanoparticles did not change the impact strength of epoxy system, 200 kg cm. After 28 cycles of UV irradiation, the impact resistance of the neat epoxy dropped down to 120 kg.cm, while that of the epoxy-CeO_2 and epoxy-Ce^{3+}/CeO_2 decreased to 140 kg.cm and 160 kg.cm, respectively (Table 2). It can be explained that the nanoparticles provided not only the UV absorption capacity, but also the hardness to the polymer matrix [20]. The epoxy-Ce^{3+}/CeO_2 had a better impact strength than the epoxy-CeO_2 because it presented much less agglomeration in the system than that of epoxy-CeO_2.
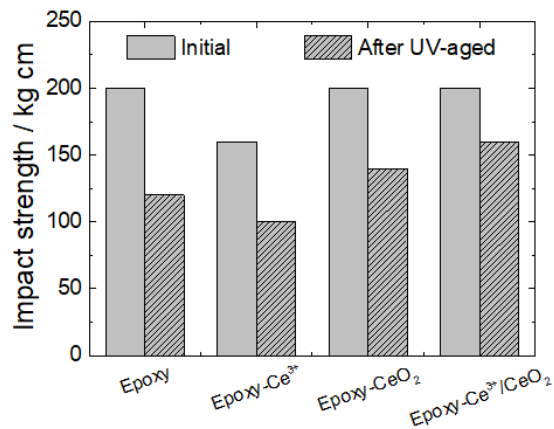
Figure 7. Comparison of impact strength obtained before and after 28 cycles of UV exposure for the epoxy coatings with and without different additives (as indicated on the figure).
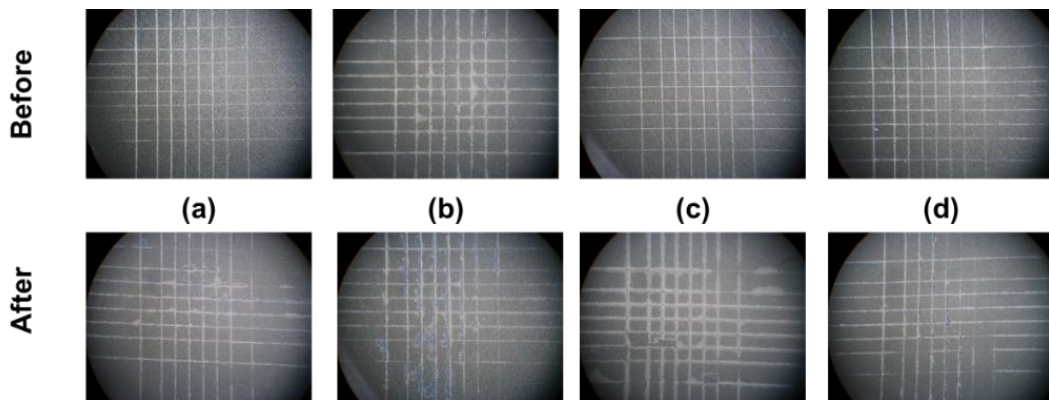

Figure 8. Optical photographs on the surface of the coatings examined by cross-cut test before and after 28 cycles of UV irradiation exposure test for neat epoxy (a), epoxy-Ce^{3+} (b), epoxy-CeO$_2$ (c), and epoxy-Ce^{3+}/CeO$_2$ (d).

Table 2. Cross-cut classification and impact resistance results for the epoxy coatings containing Ce^{3+}, CeO$_2$, Ce^{3+}/CeO$_2$ and neat epoxy coating.

Sample	Cross-cut classification		Impact strength (kg cm)	
	Before aged	After aged	Before aged	After aged
Epoxy	5B	4B	200	120
Epoxy-Ce^{3+}	4B	3B	160	100
Epoxy-CeO$_2$	5B	4B	200	140
Epoxy-Ce^{3+}/CeO$_2$	5B	4B	200	160

To examine the behavior at the interface substrate/coatings in the UV degradation exposure, the cross-cut teste was carried out (Fig. 8). Before UV degradation test, the coatings

with and without nanoparticles had a good adherence property with 5B level (Table 2). After 28 cycles of UV exposure, despite of the presence of a little more delamination around the scratch, the coating containing CeO_2 nanoparticles could reach 4B level like the neat epoxy and the epoxy-Ce^{3+}/CeO_2. The results demonstrate that the presence of the inorganic nano-compound did not clearly affect to the interaction at interface between substrate and organic matrix.

4. CONCLUSIONS

This work had examined the effect of Ce (III) ions-activated CeO_2 nanoparticles on the surface morphology, barrier and mechanical properties under UV irradiation exposure. The comparison between CeO_2 and Ce^{3+}/CeO_2 has been taken into account along in this study. After 28 cycles of UV exposure test, the epoxy coating containing activated nanoparticles had less discoloration with the decrease of 3 % lightness and of 9.5 % total color difference; better barrier property with the impedance module of 2.1×10^7 Ω cm^2 at 10 mHz; and better impact resistance with 160 kg.cm. It was also shown that although the CeO_2 and activated CeO_2 were not compatible to organic matrix, it did not affect on the adherence property of epoxy matrix.

REFERENCES

1. Wicks Z. W., Jones F. N., Peppas S. P. - Organic coatings: Science and Technology volume 1: film formation, components and appearance, Drying Technology **11** (6) (1993) 1477, DOI: 10.1080/07373939308916913

2. Cheng Y. F., Norsworthy R. - Pipeline coatings, NACE International: E-Publishing, 2016.

3. Trinh A. T., Nguyen T. T., Thai T. T., To T. X. H., Nguyen X. H., Nguyen A. S., Aufray M., Pebere N. - Improvement of adherence and anticorrosion properties of an epoxy-polyamide coating on steel by incorporation of an indole-3 butyric acid-modified nanomagnetite, J. Coat. Technol. Res. **13** (3) (2016) 489-499.

4. Luciano G., Brinkmann A., Mahanty S., Echeverrí M. - Development and evaluation of an eco-friendly hybrid epoxy-silicon coating for the corrosion protection of aluminium alloys, Progress. Org. Coat. **110** (2017) 78-85.

5. Pourhashem S., Vaezi M. R., Rashidi A., Bagherzadeh M. R. - Exploring Corrosion Protection Properties of Solvent Based Epoxy-Graphene Oxide Nanocomposite Coatings on Mild Steel, Corros. Sci. **115** (2017) 78-92.

6. Nguyen T. D., Tran B. A., Vu K. O., Nguyen A. S., Trinh A. T., Pham G. V., To T. T. X., Phan M. V., Phan T. T. - Corrosion Protection of Carbon Steel Using Hydrotalcite/Graphene Oxide Hybrid, J. Coat. Technol. Res. **16** (2) (2019) 585-595.

7. Gojny F. H., Wichmann M. H. G., Fiedler B., Kinloch I. A., Bauhofer W., Windle A. H., Schulte K. - Evaluation and identification of electrical and thermal conduction mechanisms in carbon nanotube/epoxy composites, Polymer **47** (6) (2006) 2036-2045.

8. Gonon F., Boudefel A. - Electrical properties of epoxy/silver nanocomposites, J. Appl. Phys. **99** (2) (2006) 024308.

9. Rivaton A., Moreau L., Gardette J. L. - Photo-oxidation of phenoxy resins at long and short wavelengths - I. Identification of the photoproducts, Polym. Degrad. Stab. **58** (1997) 321-332.

10. Malshe V. C., Waghoo G. - Chalk resistant epoxy resins, Prog. Org. Coat. **51** (2004) 172-180.

11. Zhang Q., Leroux F., Tang P., Li D., Feng Y. - Low molecular weight hindered amine light stabilizers (HALS) intercalated MgAl-Layered double hydroxides: Preparation and anti-ageing performance in polypropylene nanocomposites, Polym. Degrad. Stab. **154** (2018) 55-61.

12. To T. X. H., Ngo T. D., Trinh A. T., Nguyen T. D., Bui V. T., Pham G. V., Thai H., Dinh T. M. T., Olivier M. G. - Effect of silane modified nano ZnO on UV degradation of polyurethane coatings, Prog. Org. Coat. **79** (2015) 68-74.

13. Nguyen T. V., Dao P. H., Duong K. L., Duong Q. H., Vu Q. T., Nguyen A. H., Mac V. P., Le T. L. - Effect of R-TiO_2 and ZnO nanoparticles on the UV-shielding efficiency of water-borne acrylic coating, Prog. Org. Coat. **110** (2017) 114-121.

14. Liu M., Horrocks A. R. - Effect of Carbon Black on UV stability of LLDPE films under artificial weathering conditions, Polym. Degrad. Stab. **75** (2002) 485-499.

15. Ghasemi-Kahrizsangi A., Neshati J., Shariatpanahi H., Akbarinezhad E. - Improving the UV degradation resistance of epoxy coatings using modified carbon black nanoparticles, Prog. Org. Coat. **85** (2015) 199-207.

16. Saranya J., Ranjith K. S., Saravanan P., Mangalaraj D., Kumar R. T. R. - Cobalt-doped cerium oxide nanoparticles: enhanced photocatalytic activity under UV and visible light irradiation, Mat. Sci. Semicon. Proc. **26** (2014) 218-224.

17. Dao N. N., Luu M. D., Nguyen Q. K., Kim B. S. - UV absorption by cerium oxide nanoparticles/epoxy composite thin films, Adv. Nat. Sci.: Nanosci. Nanotechnol. **2** (2011) 405013-405016.

18. Nguyen A. S., Nguyen T. D., Thai T. T. - Evaluation of the anticorrosion of waterborne epoxy coatings containing cerium salt-activated ceria nanoparticles deposited onto carbon steel substrate, Vietnam J. Sci. Technol. **56** (3B) (2018) 96-103.

19. Kumar S., Srivastava M., Singh J., Layek S., Yashpal M., Materny A., Ojha A. K. - Controlled synthesis and magnetic properties of monodispersed ceria nanoparticles, AIP Adv. **5** (2) (2015) 027109.

20. Deka B. K., Maji T. K. - Effect of TiO_2 and nanoclay on the properties of wood polymer nanocomposite, Compos. Part A Appl. Sci. Manuf. **42** (12) (2011) 2117-2125.